Feasibility study of a diesel-powered hybrid DMU

Rail. Eng. Science
https://doi.org/10.1007/s40534-021-00241-2

Feasibility study of a diesel-powered hybrid DMU

Matteo Magelli[1] · Giuseppe Boccardo[1] · Nicola Bosso[1] · Nicolò Zampieri[1] · Pierangelo Farina[2] · Andrea Tosetto[2] · Francesco Mocera[1] · Aurelio Somà[1]

Received: 5 February 2021 / Revised: 14 May 2021 / Accepted: 14 May 2021

Abstract Nowadays, the interest in hybrid vehicles is constantly increasing, not only in the automotive sector, but also in other transportation systems, to reduce pollution and emissions and to improve the overall efficiency of the vehicles. Although railway vehicles are typically the most eco-friendly transportation system, since commonly their primary energy source is electricity, they can still gain benefits from hybrid technologies, as many lines worldwide are not electrified. In fact, hybrid solutions allow ICE-powered (internal combustion engine) railway vehicles, such as diesel multiple units (DMUs), to operate in full-electric mode even when the track lacks electrification. The possibility to switch to full electric mode is of paramount importance when the vehicle runs on urban or underground track sections, where low or zero emission levels are required. We conduct the feasibility study of hybridization of an existing DMU vehicle, designed by Blue Engineering S.r.l., running on the Aosta–Torino Italian railway line, which includes a non-electrified urban track section and an electrified underground section. The hybridization is obtained by replacing one of the diesel generators installed on the original vehicle with a battery pack, which ensures the vehicle to operate in full-electric mode to complete its mission profile. The hybridization is also exploited to implement a regenerative braking strategy, which allows an increase in the energetical efficiency of the vehicle up to 18%. This work shows the sizing of the battery pack based on dynamic simulations performed on the Turin underground track section, and the results demonstrate the feasibility of the hybridization process.

Keywords Hybrid railway vehicle · Energy saving · Regenerative braking · Diesel multiple unit · Lithium battery

1 Introduction

At present, the concerns about global warming and environmental pollution demand a great research effort and the involvement of government policies in order to battle climate change and its tragic consequences. The transport sector has become largely responsible in terms of CO_2 emissions and energy consumption. Rail transport is one of the most eco-friendly modes of transportation, and the specific energy consumption in rail transport has decreased by 37% between 1990 and 2013 [1]; however, it still has a great potential for emission reductions and energy savings [2], as the European Rail Industry (UNIFE) confirms that a huge amount of energy can be saved in the railway sector, especially in light rail vehicles (LRVs) and in diesel multiple units (DMUs) trains [3]. Due to the low electrification of railway networks, some countries widely adopt diesel-electric railway vehicles since they are the most diffused technical solution to run along non-electrified sections. However, dual-mode railway vehicles can work in full electric mode only in track sections where a catenary or a third rail is available. Although over the last years, electric railway vehicles have been increasingly introduced

✉ Nicola Bosso
nicola.bosso@polito.it

[1] Department of Mechanical and Aerospace Engineering, Politecnico di Torino, Corso Duca degli Abruzzi 24, Turin, Italy

[2] Blue Engineering S.R.L., Via Albenga 98, Rivoli, Turin, Italy

Published online: 11 June 2021

worldwide, it is important to improve their efficiency and to reduce losses of power supply grids because a large part of that electricity is still produced using conventional fossil sources. According to a UIC-UNIFE technical document [4], the following remarkable energy efficiency improvements can be applied on DMU trains, namely (i) energy efficiency train operation (EETROP) system, (ii) trackside energy storage systems (ESS), (iii) on-board ESS, (iv) waste heat recovery and (v) hybrid propulsion with permanent magnet synchronous motors. From the vehicle-side perspective, different options are available to improve the efficiency of railway vehicles, with regenerative braking (RB) seeming the most promising and effective one since it can theoretically provide up to 30% of the overall traction-energy demand, resulting in higher efficiency of rail vehicles and lower greenhouse gas (GHG) emissions [5, 6]. RB is a process able to harvest the part of the vehicle kinetic energy, saving it for later use, for example for re-accelerating the vehicle or feeding auxiliary equipment, by taking advantage of an electric motor behaviour to act as a generator [7]. According to Jiang et al. [8], CO_2 emissions can be reduced by 15% and 30% when RB is applied to intercity trains and suburban commuter trains, respectively. On the other hand, RB is not very effective at low speeds and mechanical braking is still required, especially in emergency operations [9].

To perform regenerative braking, a suitable ESS must be identified and adopted. Both stationary (SESS) and on-board (OESS) solutions are currently used in the railway field; however, OESS systems seem the most promising, effective, feasible and valuable method.

Currently, the most common ESS technologies for braking energy recovery in the railway field are batteries, supercapacitors, and flywheels [10], although interest in fuel cells (FC) and superconducting magnetic energy storage (SMES) is growing, but these last two technologies are still not widely adopted.

Ni-MH batteries were installed on twenty catenary-free Alstom Citadis-302 LRVs operating in Nice [11, 12], while 16 GIGACELL® Ni-MH battery modules developed by Kawasaki Heavy Industries were tested on the battery-driven SWIMO-X® running on the experimental track in Sapporo from December 2007 to March 2008, proving that 10 km could be covered in battery mode [13]. SIEMENS developed the SITRAS-HES® power unit comprising a GIGACELL® module and supercapacitors, which found its application in AVENIO vehicles running in Lisbon and Doha, able to operate without being supplied from other power sources [14, 15].

Another type of battery adopted in the railway field is Li-Ion battery (LIB). Applications include the so-called Twilight Express Mizukaze, equipped with LMO (lithium manganese oxide) battery from the LIM series by GS Yuasa, able to travel in the non-electrified section of the Japanese Sanin Main Line [16], as well as the vehicles developed from the collaboration between Hitachi Ltd. and the East Japan Railway Company, namely the JR Kyushu Series BEC819, based on a battery drive system, and the JR East Series HB-E210 and HB-E300, exploiting a hybrid drive system [17]. Furthermore, the collaboration between Bombardier Transportation and UK Network Rail led to the design of the new Electrostar class 379, running on the Essex line [18], which is the first UK battery-powered train, also called independently powered electric multiple unit (IPEMU) since it can be powered from catenary in electrified sections and from a large battery pack in non-electrified tracks.

With respect to batteries, supercapacitors (or electric double-layer capacitor, EDLC) feature higher energy density, capacity and charge/discharge speed, as well as a high lifecycle and efficiency [19]. From 2003 to 2007, a remarkable application of supercapacitors for the recovery of braking energy involved Bombardier Transportation that developed the MITRAC® Energy Saver, an OESS that enabled a prototype LRV, operative in Mannheim (Germany), to save up to 30% of traction energy [20]. Some vehicles of the existing Series 313 operating on the Japanese Chuo line were retrofitted and equipped with 570 EDLC cells, achieving 1.6% of energy saving compared to the non-retrofitted vehicles [21]. Moreover, Alstom and RATP (a public transport operator) have collaborated in the STEEM project that aims to improve the energy efficiency of railway vehicles. As result of the project, an EDLC-equipped Citadis vehicle was launched on the tramway T3 of Paris, in late 2009. The STEEM vehicle is normally powered by overhead contact line and uses EDLC bank for a distance of 300 m, achieving daily energy reduction of 13% [22]. A more detailed list of EDLC-equipped railway vehicles can be found in the work by Swanson and Smatlak [15], which shows that most applications concern vehicles running on tracks no longer than some hundreds of metres.

Despite the simple design and the maturity of the technology [23–25], flywheels are not widely adopted as ESS in the railway field, but a few applications and feasibility studies are still witnessed. Advantages of flywheel technology are long lifecycle (hundreds of thousands of cycles), very low maintenance, long calendar life and high capability to transfer high power within few seconds. In addition, since power and energy ratings of the flywheel are independent, each of them can be optimized taking into account specific application requirements. On the other hand, flywheels have high self-discharge and up to 20% of the stored energy can be lost within one hour; furthermore, flywheel rotors can be hazardous if not well designed. A remarkable flywheel trackside application is proposed in [26] showing improvements of energy efficiency up to

21.6% and 22.6% for single and multiple trains, respectively, while in South Korea flywheels were installed for peak power reduction purposes on the Panam–Banseok line, achieving peak reduction up to 36.7%, an energy saving of 48 MWh, as well as financial improvement of 24,000 $/month [27]. Feasibility simulations showed that the installation of flywheels on LRVs can bring benefits in terms of energy savings and reduction of fuel consumption and CO emissions [28, 29].

The present paper is a feasibility study for the improvement of the energy efficiency of an existing DMU vehicle designed by Blue Engineering S.r.l. Several options were investigated, including heat recovery from exhaust gases either for electrical energy production through steam or organic rankine cycle (ORC) or to produce hot water, which may feed thermal loads such as HVAC (heating, ventilation and air conditioning) units or a radiant floor system. Nevertheless, these solutions were discarded because they would allow a limited energy recovery despite requiring significant changes in the current DMU train configuration. Therefore, the most suitable solution to obtain remarkable energy savings was RB. The existing DMU train uses dynamic braking to slow down from high speeds; however, the surplus of kinetic energy of the vehicle that does not feed auxiliary equipment is dissipated into heat through resistor banks (rheostatic banking). The proposed upgrade deals with the replacement of the original power pack with a new power unit including an OESS. The chosen OESS is an LTO (lithium titanate oxide) battery, due to the high C-rates, life cycle of more than 5000 cycles, fast charging time and a large range of operating temperatures. Therefore, the proposed changes lead to a hybridization [30–33] of the original vehicle, which differs from typical dual-mode trains in its capability to work in full electric mode even when no catenary or third rails are installed on the track, also reducing emissions and fuel consumptions, as required in underground and urban sections. Moreover, the proposed hybridization can be exploited in very cold areas, where extremely low temperatures can damage the electrical contacts.

2 Case study

The reference vehicle adopted in this work is an existing DMU train designed by Blue Engineering S.r.l. The vehicle comprises four wagons distinguished into two types called car 2 and car 4, head and body of the trainset, respectively. The diesel generator, HVAC units and brake resistor bank are roof-mounted as shown in Fig. 1. Essentially, the heating/cooling system of car 2 differs from the one of car 4 in the HVAC unit installed in the driver's cabin.

Both car types are equipped with electro-dynamic (ED) and pneumatic braking systems: the former operates in normal braking operation, whereas the latter is activated at a very low speed, in emergency operations or in case of failure of ED braking system. In fact, during braking manoeuvres, the control unit sends a braking signal to a traction converter that enables the motor to act as a generator, applying a resistant torque to the wheelsets of the motor bogie. The existing vehicle was designed so that, during the braking phase, the part of the ED braking power feeds auxiliary equipment, while the exceeding part is wasted through the brake resistor bank. Each brake resistor bank has a rated power of 340 kW and a mass of about 360 kg. Once the vehicle reaches a very low speed (i.e., in the proximity of the station), the control unit activates pneumatic braking system ensuring short braking distance despite its high operational costs in terms of pad and disc wear and energy waste. The main data of the original DMU are summarized in Table 1.

Each car of the DMU is equipped with its own diesel generator, and there are not any other external power supply systems; thus, the diesel engine plays an essential role for the proper functioning of the whole system. However, because of safety issues, the vehicle is developed so that it is capable of completing its mission even in case of failure of two of the four diesel engines. The power pack weighs about 8 tons and includes a diesel engine coupled to the electric generator (diesel generator), a control and monitoring system, a fire fighting system and a cooling system.

The power pack provides power to the following elements: the traction converter, an auxiliary converter (medium voltage (MV) loads) and to a battery charger (low voltage (LV) loads). More in detail, the diesel generator supplies power to a rectifier that converts alternating current (AC) into direct current (DC). Then, power flows to traction and auxiliary converters and to the battery charger. The traction converter again converts DC–AC, supplying power to traction motors. The control unit is based on a PID controller and sends a signal to the traction converter that regulates ED braking and traction efforts by means of a VVVF inverter. The auxiliary converter feeds and regulates the power of the MV loads such as HVAC units, compressors and other auxiliary systems, whereas the battery charger supplies power to the existing backup battery pack used in start-up and emergency operational mode.

Figure 2 shows vehicle power flow in different operational modes synthetized as follows:

- Traction: the vehicle accelerates until reaching cruise speed. During this phase, electric motors need to provide the maximum torque, and thus, they demand the maximum power because of the inrush current.

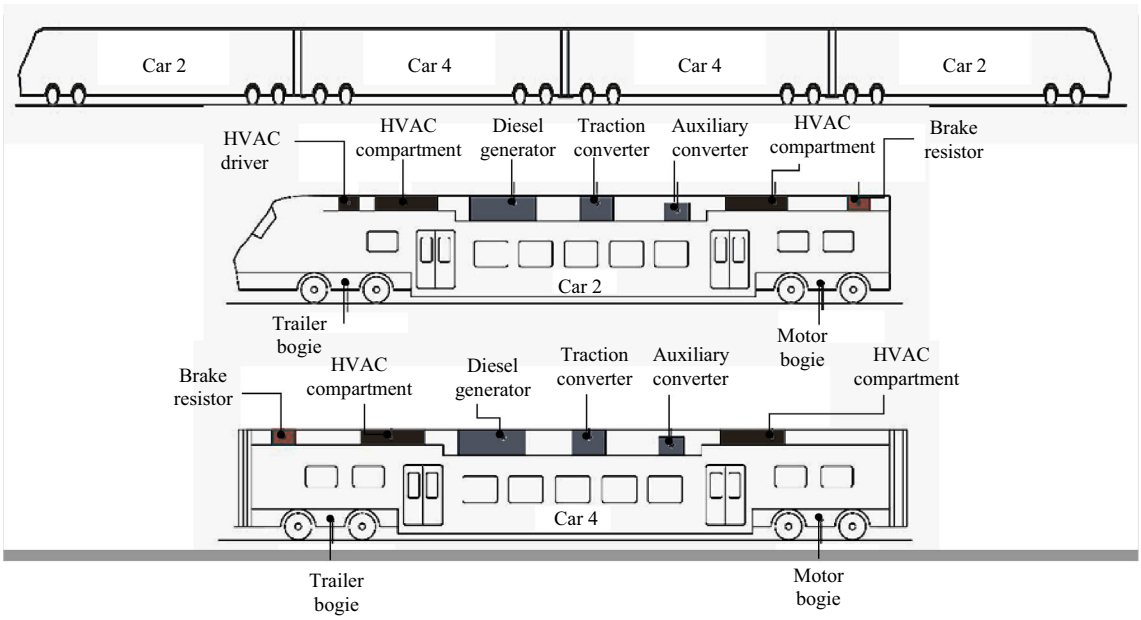

Fig. 1 Roof-mounted equipment in head and body wagons

Table 1 Heads and body wagon characteristics

Characteristics	Head	Body
Length/height/width (m)	27.18/4.28/2.82	25.72/4.28/2.82
Wheel diameter (mm)	920	920
Track gauge (mm)	1,435	1,435
Boogie wheelbase (mm)	2,500	2,500
Nominal Boogie centre spacing (m)	19	19
Axle load (t/axle)	18	18
Number of axles	4	4
Primary power source: diesel engine (kW)	560	560
Transmission system: electric motor (kW)	180 × 2 units	180 × 2 units
Maximum speed (km/h)	120	
Wheel arrangement	(2B)(22) (22)(B2)	
Layout	Driver's cabin and passenger compartment	Passenger compartment
Capacity (persons)	228	201
Electric motors (kW)	2 × 180	2 × 180
Compressors (kW)	7.5	7.5
Compartment HVAC units (kW)	24 × 2	24 × 2
Driver HVAC unit (kW)	5.8	–
220 V sockets (kW)	2	2
Power pack cooling system (kW)	18	18
Total (kW)	435.5	441.3

Once the vehicle reaches cruise speed, electric motors only need to overcome drag force and their power demand decreases. In this phase, the diesel generator needs to provide power to auxiliary equipment and electric motors (see Fig. 2a).

- Coasting: vehicle runs by inertia and slowly decreases its velocity. The diesel generator provides power to auxiliary equipment only (see Fig. 2b).
- Braking: when the vehicle is decelerating, initially ED braking energy is applied by means of the VVVF (variable voltage and variable frequency) inverter that

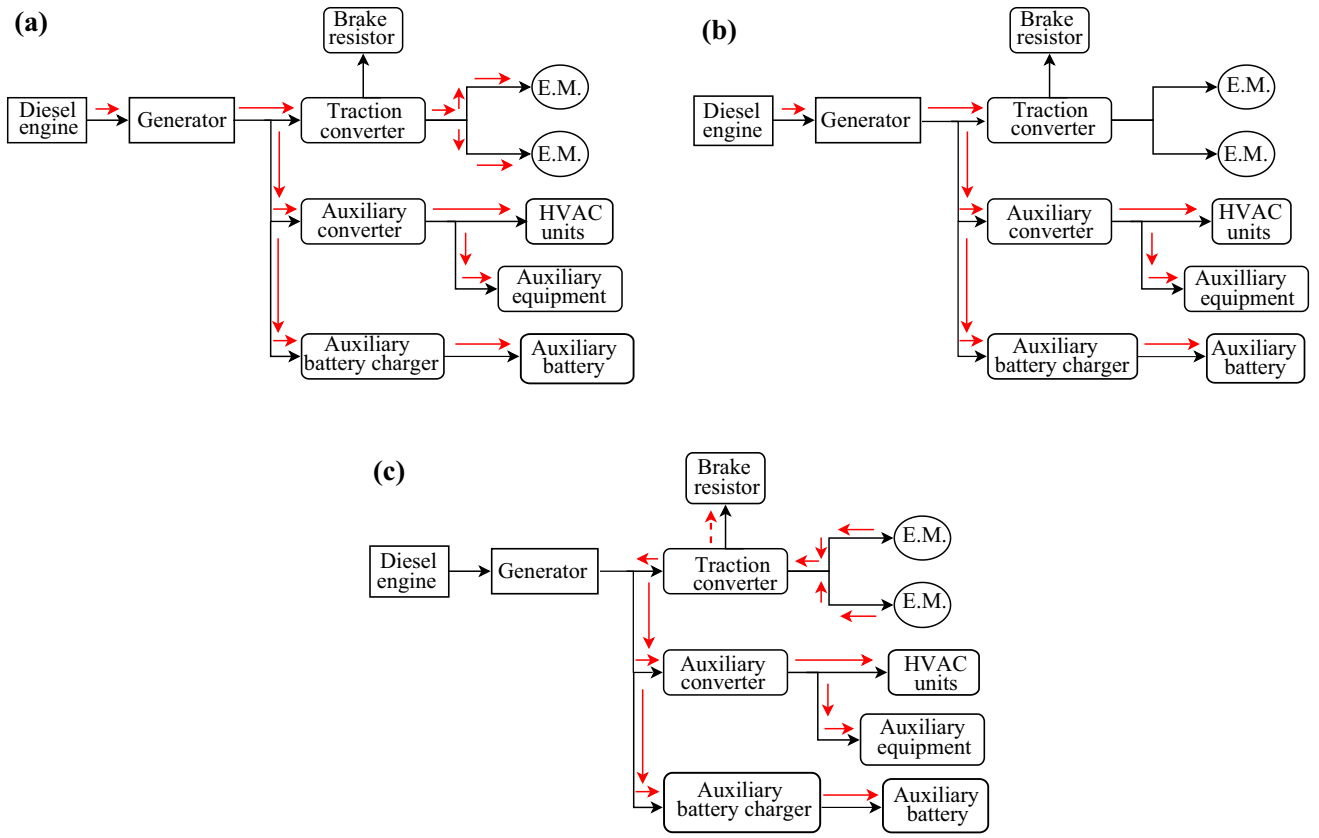

Fig. 2 Power flow of the single car: **a** acceleration phase, **b** coasting operation, and **c** ED braking

enables electric motors to act as generators. In this case, a fraction of the generated energy is used by HVAC units and auxiliary equipment (see Fig. 2c). Since the original vehicle does not include an ESS system for energy storage, the surplus of energy is wasted by the resistor bank.

The hybridization of the existing vehicle essentially deals with the substitution of one of the four existing diesel engines with the OESS. Besides allowing ED braking energy recovery, this choice enables the vehicle to operate in a wider operation range (i.e., underground section) and to reduce pollutant emissions in critical areas, such as not electrified urban stations. Based on these considerations, the OESS was designed to satisfy the power demand of the vehicle during the entire urban track described next.

Figure 3 conceptually shows the hybridization idea, which is applied to the existing DMU model. The retrofitted trainset will then have three diesel generators and one battery pack that shall allow the vehicle to recover ED braking energy as well as to reach non-electrified urban stations and to operate in underground tracks where diesel generator use is forbidden.

Dual-mode vehicles are already available on the market and exploit the same operating principle of the retrofitted vehicle presented in this work. In fact, dual-mode vehicles use diesel generator in non-urban areas, whereas in the proximity of urban stations or in underground tracks, they use an electrical power supply, such as a pantograph that powers the vehicle through overhead catenary. This double-power supply system is relatively new and quite diffused in the railway sector, but the vehicle is still dependent on the presence of a track electrical grid that is generally not ensured everywhere. On the contrary, the proposed retrofitted hybrid vehicle will be capable of travelling independently in non-electrified urban and underground areas thanks to the OESS. In addition, in dual-mode vehicles, regenerative braking takes place only when a close vehicle requires power at the same time, and this scenario is almost impossible in systems different from funicular railway or similar. Moreover, the retrofitted vehicle, through the OESS, could use the engine at optimal efficiency point, reducing its pollutant emissions.

The vehicle was designed to operate the service on the Aosta–Torino railway line, which is partially electrified. In particular, the Aosta railway station is not electrified, and it is in proximity of the city centre. For this reason, the adoption of a hybrid railway vehicle can significantly reduce pollution, especially during the winter months. Moreover, the railway line includes underground and non-

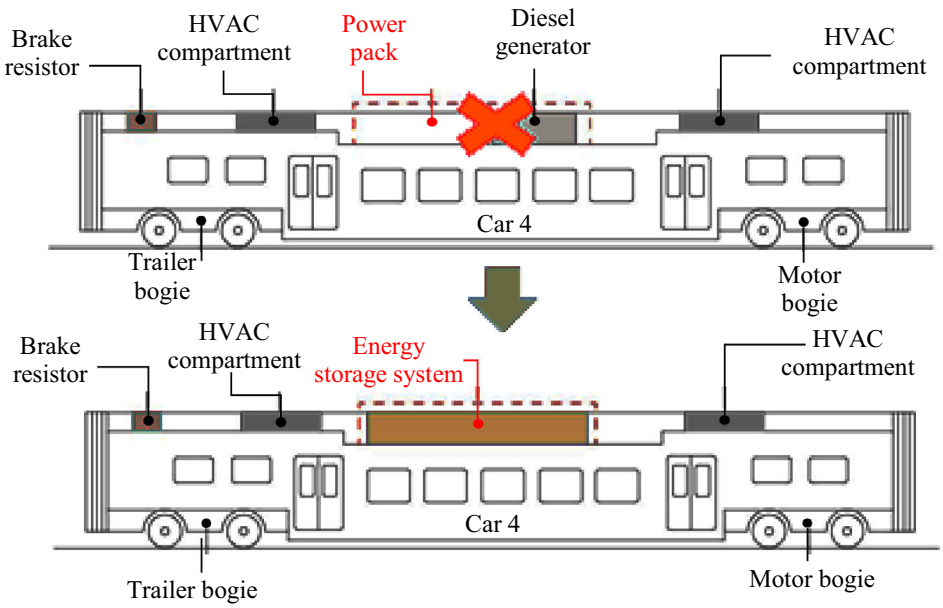

Fig. 3 Conceptual scheme of the hybridization process

underground sections in the urban area of Turin for a length of about 20 km, in the track section connecting the stations of Torino Rebaudengo Fossata, Torino Porta Susa and Torino Porta Nuova. In these sections, the use of the diesel generator is forbidden, and the vehicle must work in full electric configuration. This condition is used to design and size the battery pack. Speed and slope profile of the track in the urban area of Turin are shown in Fig. 4. Once the vehicle reaches Porta Nuova railway station, acceleration and slope profiles are reversed because the track involves a round trip starting from the beginning of the underground section, located at the entrance of Turin (station of Rebaudengo Fossata), to the central station of Porta Nuova. Therefore, the vehicle stops twice at each station, i.e., Rebaudengo Fossata (Reb), Porta Susa (PS) and Porta Nuova (PN), with the way back highlighted in Fig. 4 using the contraction "(R)". The departure from each station in both ways is identified by the abbreviation "Dep." As a side note, it should be known that the speed profile is imposed and controlled by the railway operator; thereby, the vehicle power demand can be easily calculated, as explained in the next section.

Based on the considerations exposed in the introduction section and on the proposed case study, the best choice for the OESS proved to be an on-board battery, which combines good power and energy density, while supercapacitors were discarded due to their low power density and flywheels were not considered suitable for the selected application since this technology is not commonly used in hybrid vehicles. More in detail, the LTO battery was selected since it guarantees a good compromise in terms of battery pack lifecycle, power density, energy density, and charging/discharging times.

3 Battery pack sizing

To calculate the vehicle power and energy demand, which are essential for the battery pack sizing, a longitudinal train dynamic (LTD) model is developed, considering slope, acceleration and speed profile of the given track shown in Fig. 4. As previously explained, the battery module is sized in order to guarantee the running of the vehicle in full electric mode in the urban area of Turin, which has a length of about 20 km.

Among other considerations, it should be highlighted that RB power represents part of the total braking effort since ED braking use is limited by the maximum braking power of motors and vehicle speed. The proposed LTD model is 1D, as common to most LTD simulators [34, 35] and as suggested by the recently established international benchmark of LTD simulators [36, 37]. The model considers both the gravitational force due to track slope and the propulsion resistance, which is the sum of rolling resistances and air resistances. The curving resistances can be neglected in this work since the considered track line can be regarded as an approximately straight line in the urban area of Turin with no tight curves. The gravitational force is easily calculated by means of

$$F_{\text{slope}} = M_{\text{veh}} g \sin \vartheta, \tag{1}$$

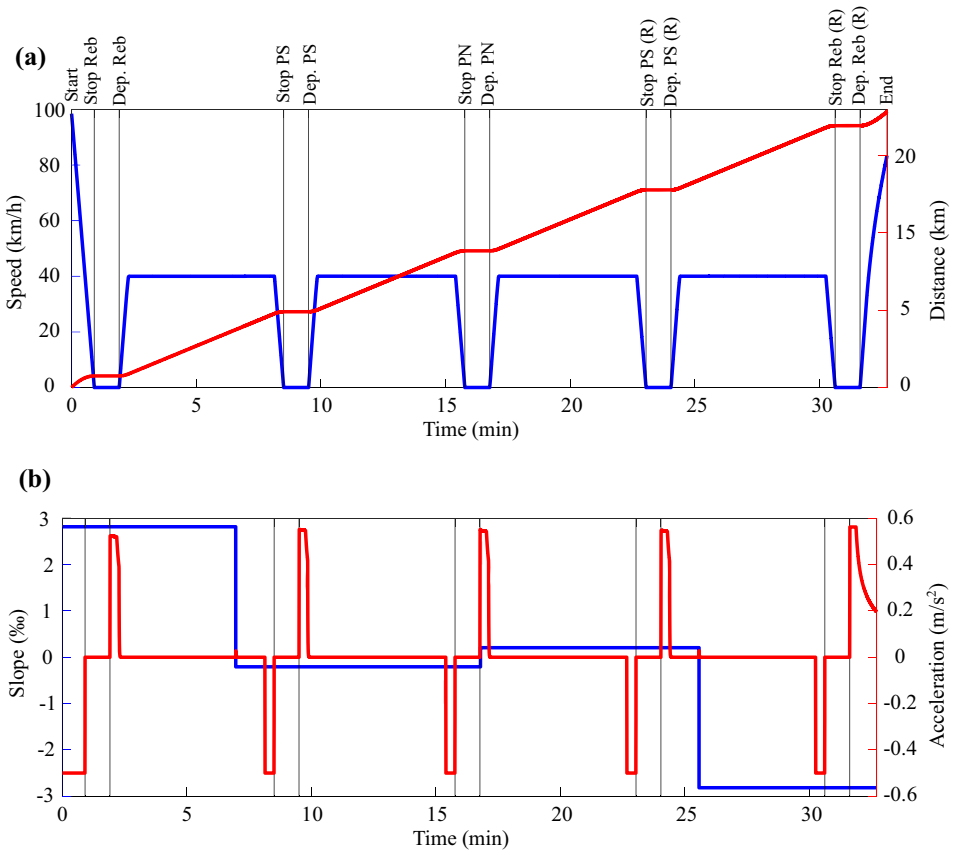

Fig. 4 Profiles of the track in the urban area of Turin, **a** speed and **b** slope

where ϑ is the track angle of inclination, M_{veh} is the total mass of the DMU train, and g is gravity (9.81 m/s^2).

Propulsion resistance F_{Res} is typically expressed by means of second-order polynomial equations as a function of the vehicle speed S_{veh}, and among different expressions witnessed in the literature [38–40], the Davis' formula is adopted in this work:

$$F_{\text{Res}} = 6.4M_{\text{veh}} + 129N_{\text{ax}} + 0.091M_{\text{veh}}S_{\text{veh}} + 0.051A_{\text{front}}S_{\text{veh}}^2, \tag{2}$$

where N_{ax} is the total number of train axles and A_{front} the train cross-sectional area.

Since the vehicle speed and acceleration profiles are known in advance, the tractive and braking effort F_{Tr} can be calculated as the sum of the forces previously described:

$$F_{\text{Tr}} = M_{\text{veh}}a_{\text{veh}} + F_{\text{slope}} + F_{\text{Res}}, \tag{3}$$

$$P_{\text{Dem}} = F_{\text{Tr}}S_{\text{veh}}, \tag{4}$$

where a_{veh} is the vehicle acceleration and P_{Dem} is the power demand.

Please note that for the sake of simplicity, the proposed model considers the vehicle coupling elements as completely rigid links, so that the speed and acceleration of each car are equal to the speed and acceleration of the whole train.

Table 2 shows the main results obtained from the application of Eqs. (1)–(4) in the case study described by the track slope, train speed and acceleration profiles presented in the previous section (see Fig. 4). Please note that the table also includes other quantities that are essential for the battery pack sizing. Due to the high power demand of the considered application, the module chosen for this application is the Toshiba battery module type 3–23, whose main technical data are summarized in Table 3, while its charging and discharging curves are presented in Fig. 5.

A preliminary sizing of the battery pack is performed according to the four steps suggested by Linden and Reddy [41]; for a first approximation of the number of modules to put in series (n_{s}) and in parallel (n_{p}), see Eqs. (5)–(8):

$$n_{\text{s}} = \frac{V_{\text{des}}}{V_{\text{mod}}}, \tag{5}$$

$$E_{\text{BP}} = \frac{E_{\text{dem}}}{\text{DOD}}, \tag{6}$$

Table 2 Data for battery pack design

Parameter	Value	Note
Total energy demand E_{dem} (kWh)	196	Including auxiliary equipment
Maximum tractive power (kW)	1,614	Electrical power
Maximum ED braking power (kW)	1,584	Electrical power
Maximum braking power (kW)	4,088	Pneumatic and electric braking
Desired voltage V_{des} (V)	950	Based on electrical requirements
Minimum voltage (V)	850	Based on electrical requirements
Power pack mass (kg)	800	–
Diesel generator power (kW)	560	One diesel generator each car

Table 3 Battery module technical data

Parameter	Value
Nominal voltage V_{mod} (V)	27.6
Capacity at C/5 C_{mod} (Ah)	45
Minimum/maximum voltage (V)	18.0/32.4
Maximum charge/discharge	160 continuous
current (A)	350 peak
Operative temperature range (°C)	− 30–45
Dimensions (mm)	190 × 361 × 125
Mass M_{mod} (kg)	15

$$C_{BP} = \frac{E_{BP}}{n_s V_{mod}}, \tag{7}$$

$$n_p = \frac{C_{BP}}{C_{mod}}, \tag{8}$$

where V_{des} is the desired voltage, V_{mod} the voltage of a single battery module, E_{BP} the energy of the battery pack, E_{dem} the demanded energy (calculated in Table 2), DOD is the battery pack depth-of-discharge, assumed equal to 80%, C_{BP} the battery pack capacity, and C_{mod} the capacity of the single module.

Once the number of parallel n_p and series n_s modules is determined, the mass of the battery pack M_{BP} is easily calculated by means of Eq. (9), in which the 1.2 multiplication factor considers the mass of auxiliary systems and M_{mod} is the mass of the single module,

$$M_{BP} = 1.2 n_s n_p M_{mod}. \tag{9}$$

By Eqs. (5)–(8), a preliminary sizing of the battery pack is obtained; however, the sizing process must ensure that during operation the required current is always below the maximum current withstood by the battery and that the system voltage is above the minimum voltage. This aspect is considered by increasing the number of parallel branches of the initial battery pack configuration until discharging/charging current complies with the battery limits, by means of a MATLAB-dedicated script. The final battery pack configuration includes 38 series modules and 12 parallel branches, which lead to a total energy of the battery pack equal to 566 kWh, a maximum discharge power (at 3C-rate and 80% state of charge, SOC) of 1,775 kW and a total mass including auxiliary equipment equal to 7,660 kg.

Please note that the replacement of the original power pack (diesel engine and accessories) with the new battery pack leads to a variation in the train mass. Calculation of the traction force and of the demanded traction power using Eqs. (1)–(4) was performed on the retrofitted vehicle; however, due to the limited mass change, below 1.5%, the demanded power is substantially unchanged.

As the project is in its feasibility phase, parameters such as battery thermal management and internal resistance are not considered. However, to estimate the dynamic behaviour of the battery pack and the amount of recovered braking energy, a dynamic measure of battery pack SOC is required during vehicle operations. Scientific literature proposes various SOC measure methods and battery mathematical models [42–46], but these methods are typically based on many parameters that are still not known at this preliminary stage of the activity. Therefore, the following main assumptions hold:

1. Braking power firstly feeds auxiliary equipment and secondarily battery pack, according to its SOC.
2. If braking power is smaller than auxiliary power demand, the battery pack should supply that power difference.
3. The internal resistance value is not provided by the battery manufacturer, so it is neglected.
4. Battery efficiency is assumed to be 90% for a charge/discharge cycle.
5. It is assumed that electric motor efficiency does not change when it acts as a motor or as a generator.
6. Auxiliary power demand is assumed to be constant and equal to 191 kW for the whole trainset.

To assess the battery pack SOC during operation, dynamic simulations are performed on the case study described in the previous section, which includes four main

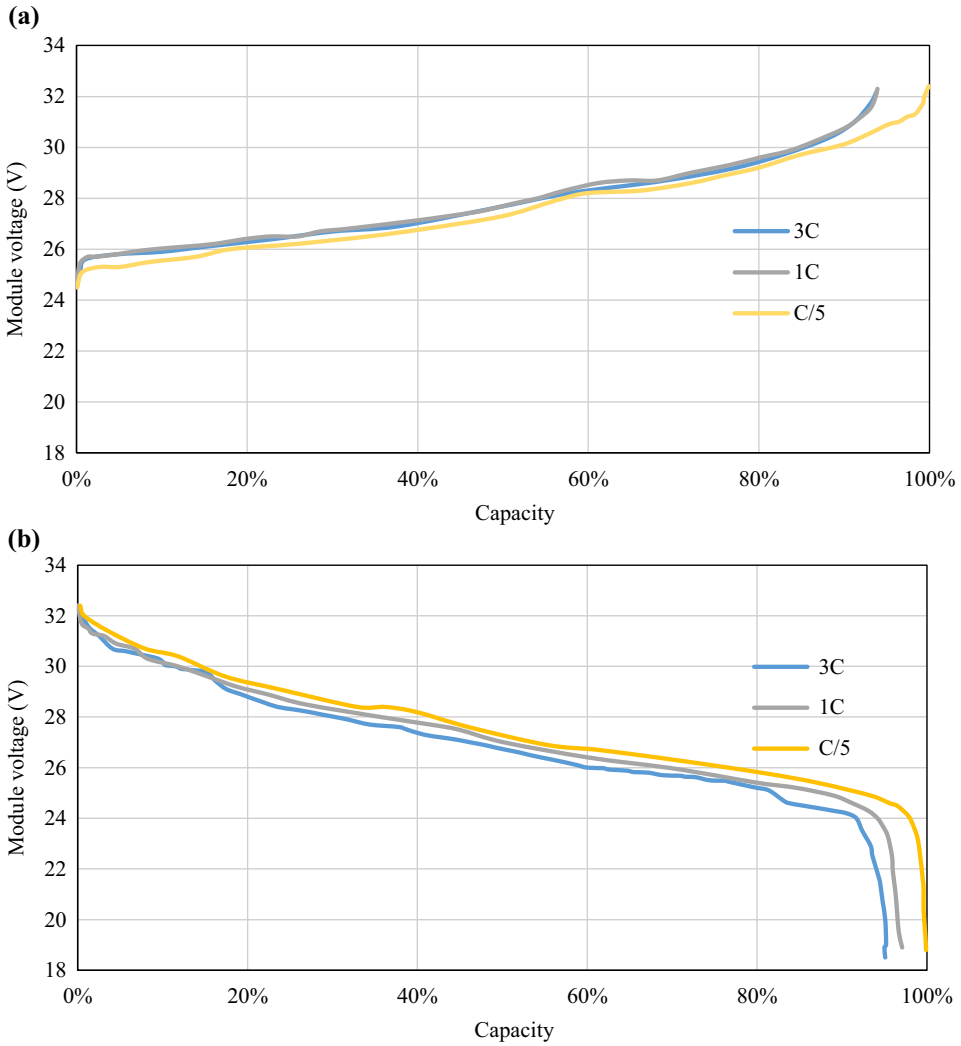

Fig. 5 Characteristics of the selected battery module for different C-rates, **a** charge and **b** discharge

Table 4 Vehicle operational modes in full electrical condition

	Traction	Coasting	Station stop	Braking
Operational mode description	The vehicle requires the maximum power since electrical motors need very high current in order to provide the maximum tractive efforts necessary in the acceleration phase	The vehicle has already reached cruise speed, and relatively small amount of power is required to the battery pack for powering auxiliary equipment and electric motors	When the vehicle is stationary, the battery pack is discharging because of auxiliary power demand	In proximity of the stations, the vehicle initially brakes through the ED braking system and the battery pack is charged according to its SOC. At very low speed, the pneumatic braking system is activated, and the vehicle rapidly reaches stationary mode
Battery pack phase	Discharging	Discharging	Discharging	Charging when braking power is larger than auxiliary power
	Positive power in the dynamic simulation	Positive power in the dynamic simulation	Positive power in the dynamic simulation	Negative power in the simulation

operational modes, namely traction, coasting, station stop and braking. Please note that the battery sizing is performed considering the vehicle working in full electric mode. Table 4 gives an overview of these four operational modes and of the related battery pack phases.

The MATLAB algorithm for the battery SOC evaluation is based on the simple Coulomb's counting method, which performs the integration of charging/discharging current over time:

$$\mathrm{SOC}_i = \mathrm{SOC}_{i-1} \pm \int_{t_0}^{t_0+\Delta t} I_i \mathrm{d}t, \tag{10}$$

$$I_i = \frac{P_i}{V_{\mathrm{BP},i}(\mathrm{SOC}_i)}, \tag{11}$$

where subscript i refers to the ith considered time step, P is power, V_{BP} is the battery pack voltage, and I is the battery pack current.

Please note that in Eqs. (10)–(11), traction and auxiliary power demands have positive value, whereas braking power is negative. Same considerations are still valid for current. Therefore, the sign of "+" in Eq. (10) applies during battery charging, while that of "–" is used for battery discharging.

The initial values of battery pack SOC as well as the power demand during the simulation are known in advance. The simulations consider different values of initial battery pack SOC. During the simulation, the battery pack voltage can be determined as a function of the current battery SOC, but the battery features a hysteretic behaviour in charging and discharging operations, which is managed in the MATLAB script by means of a proper approach based on the energy conservation principle, allowing the logic switch between the charging (f_{crg}) and discharging (f_{discrg}) functions. Figure 6 shows a flowchart of the MATLAB algorithm implemented for the evaluation of the battery pack SOC during dynamic simulation, where SOD denotes battery of discharge, I_{crg} charging current, and $I_{\mathrm{maxallowed}}$ maximum allowed charging current.

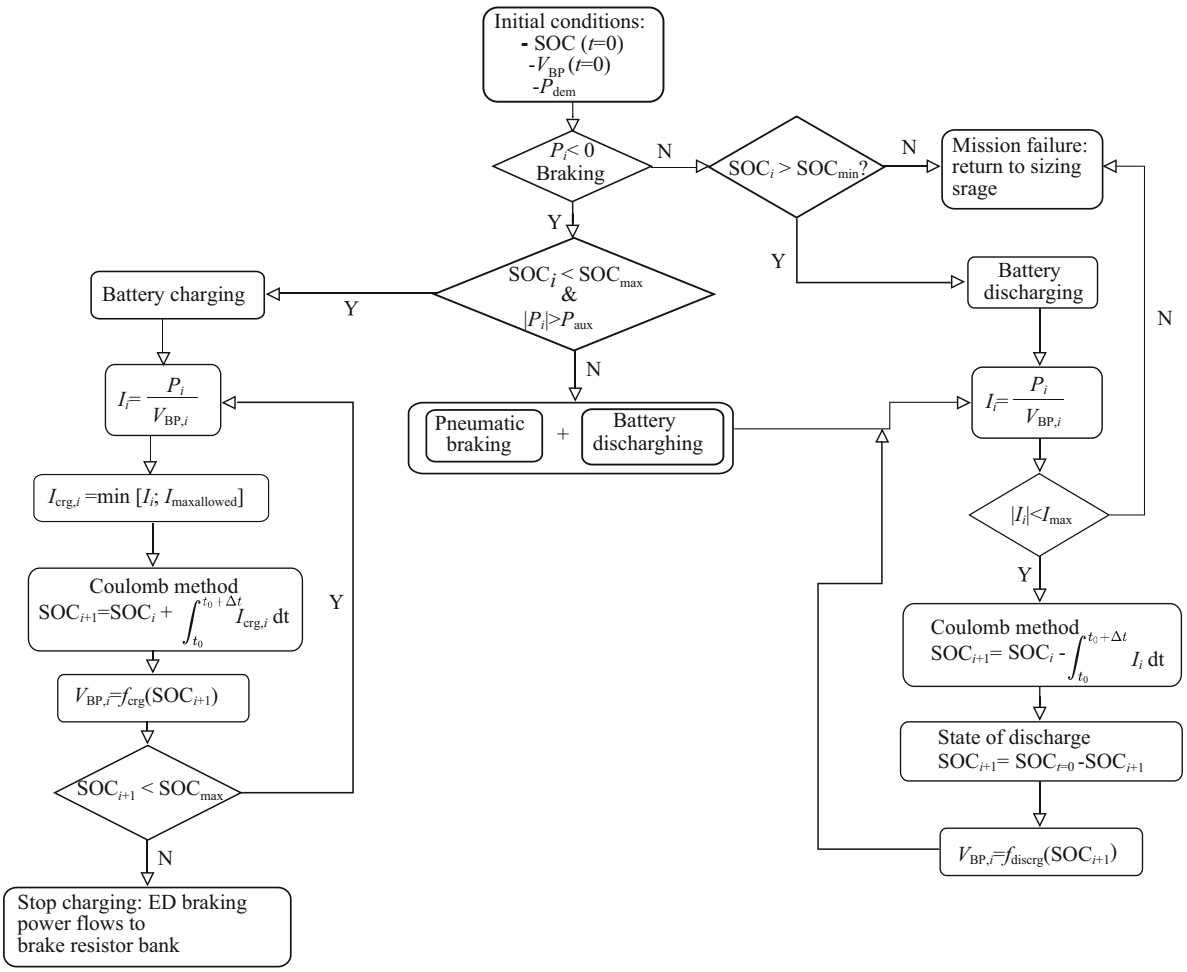

Fig. 6 Flowchart of MATLAB algorithm for dynamic simulations

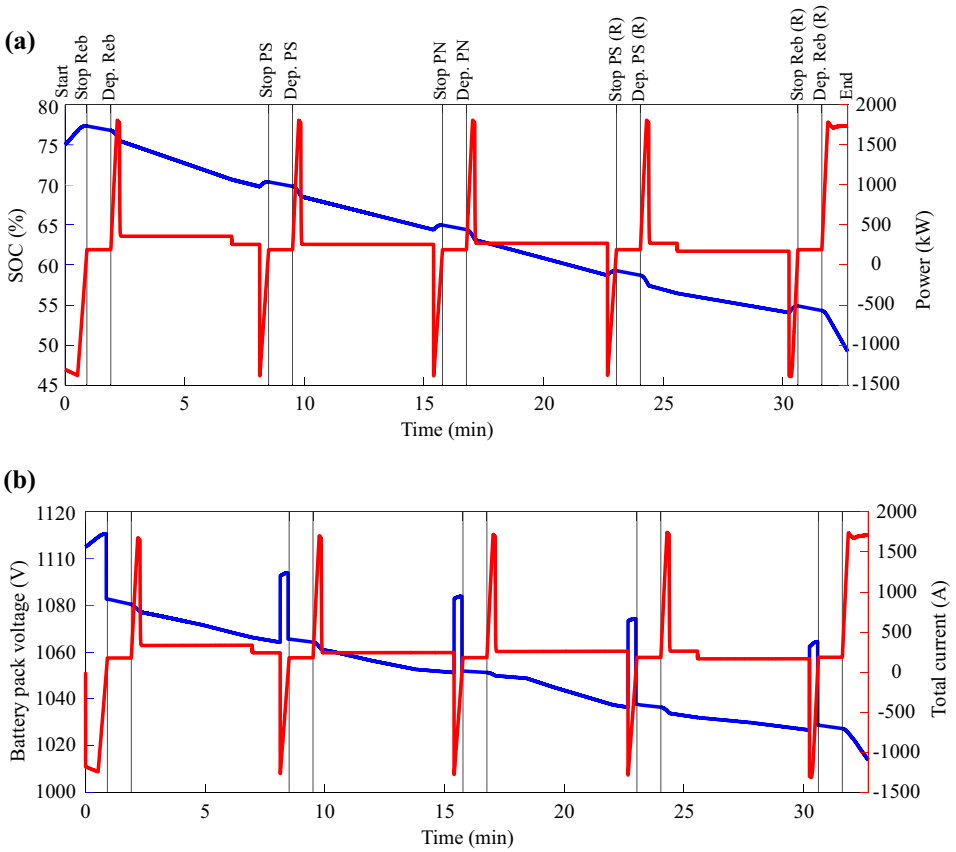

Fig. 7 Dynamic simulations: **a** SOC and power, and **b** battery pack voltage and total current

4 Results and discussion

The dynamic simulations aim to estimate the amount of regenerative energy recovered through the battery pack and to evaluate the evolution of the electrical parameters for ensuring the compliance with basic electrical requirements, such as maximum current and minimum voltage. Since the performed dynamic simulation neglects factors that, in the real application, could negatively affect battery pack performance, it is essential to satisfy at least electrical, size and weight requirements for the hybridization project to be considered feasible.

As shown in Fig. 7a, the SOC level slightly increases at every braking event and linearly decreases in the rest of the journey when no braking effort is applied. Additionally, in the graph of Fig. 7b, it is possible to identify regenerative braking events that take place when the current becomes negative and the voltage has a quick rise, due to the activation energy required by the battery to reverse the lithium-ions flow when the transition from discharging to charging mode occurs. Moreover, it should be noted that the current essentially has the same trend of power demand because of the calculation method.

As expected, the SOC value drastically decreases when the vehicle departs from each station, since in traction mode the vehicle requires the maximum power from the battery pack that, consequently, is forced to provide a high current. The results of the dynamic simulation presented in Fig. 7 also demonstrate that the SOC level remains in the range of acceptable values since the vehicle terminates its mission with battery pack SOC about 50%, considering an initial SOC of 75%.

The initial value of SOC strongly affects the amount of recovered energy as well as charging time; in fact, SOC values higher than 90% should be avoided; otherwise, charging time could take too long. On the contrary, if the battery reaches a very low SOC level, the voltage dramatically drops, thus jeopardizing the compliance with the basic electrical requirement and exceeding the maximum current allowed by the battery pack. Additionally, the high currents could generate heat so quickly that the battery thermal management system might not be able to handle it, thus leading to battery pack failure.

Several simulations were performed considering different values of the initial SOC, and the corresponding regenerative energy calculated for each scenario is presented in Fig. 8, which shows that the total amount of

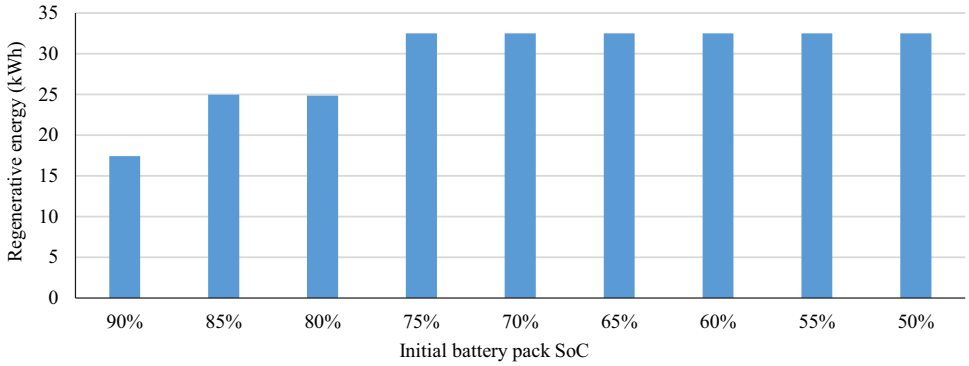

Fig. 8 Regenerative energy as a function of initial SOC

regenerative energy has an upper limit due to vehicle's kinetic energy, as the amount of recovered energy is approximately constant below a certain value of the initial SOC. On the other hand, the recovered energy decreases as the initial SOC level increases, due to the battery restriction to accept high current above a certain SOC value.

The results of the simulations performed considering different values of initial SOC highlighted that the regenerative braking can lead to recover up to 18% of the total energy demand, which corresponds to approximately 85% of the total ED braking energy, thus proving to be a very promising strategy for enhancing the energy efficiency of the railway vehicle. Additionally, the best compromise between energy recovery and charging time was achieved for the initial SOC values in the range of 65%–75%. In fact, large depth-of-discharge values should be avoided, since they strongly affect the battery life and state of health.

A second set of dynamic simulations was run to assess the vehicle performance in case of absence of regenerative braking operations, to obtain a safe range of SOC level within which the vehicle is able to complete its mission. The results showed that the vehicle should have an initial battery charge higher than 55% to guarantee the mission completion, while for the initial SOC levels below 55%, the battery pack would reach an unacceptable SOC value at the end of the mission.

Finally, from the two sets of dynamic simulations, it can be concluded that an initial SOC value between 55% and 75% ensures the completion of vehicle mission as well as optimal braking energy recovery.

5 Conclusions

This work deals with the retrofitting and hybridization of an existing DMU to improve the vehicle energetical efficiency. The most promising solution to achieve this goal in the considered case study proves to be the energy recovery by means of regenerative braking, which is possible thanks to the electrical transmission system fitted on the vehicle. However, since the vehicle is not equipped with a secondary power supply system (i.e., third rail or pantograph), the only way to recover ED braking energy is the installation of an OESS that, also, allows the vehicle to handle regenerative energy with no regard to grid capacity of accepting power. As a result of the research activity done, the lithium battery seems to be the most suitable energy storage technology for this type of application characterized by very high-power demand and current. Among the wide range of lithium battery chemistries, the LTO-based battery proves to be the most suitable because of their short charging time, long lifecycle, wide range of operating temperatures and high C-rate. The replacement of the original power pack with a battery pack also enables the vehicle to operate in full electric mode. Therefore, the retrofitted vehicle is a hybrid vehicle, which differs from typical dual-mode trains since it has no need for external electrical power supply in underground and urban tracks.

Dynamic simulations performed on the round trip between the stations of Torino Rebaudengo and Torino Porta Nuova on the Aosta-Torino Italian line led to encouraging outcomes, as the retrofitted vehicle can recover up to 18% of the total energy demand and almost 85% of the total ED braking energy. Moreover, the results showed that the vehicle energetical performance is strictly dependant on the initial SOC of the battery pack, as the vehicle can complete the mission if the initial SOC is above 55%, with a good compromise between the maximum recovered energy and recharging time when the initial SOC is in the range of 55%–75%.

The proposed hybrid architecture gives an important contribution for the reduction of local concentration of particulate and CO2 emissions, which are a major concern in the city of Turin. Furthermore, the retrofitted hybrid DMU railway vehicle generates secondary improvements

such as extending applicability field of the vehicle and using the battery pack as acceleration booster. Additionally, by comparing the retrofitted vehicle with common dual-mode railway vehicles, the first has the advantage of being independent from the electrical grid and this should largely increase positive effects of regenerative braking, reducing the vehicle fuel demand.

In future works, a more precise estimation of the retrofit process feasibility could be obtained by developing a model of the battery pack control electronics and thermal management system, which is neglected at this initial stage of the activity. Moreover, better performances could be achieved by combining the proposed battery module with a high specific power technology. Finally, upgrades of the activity should face the challenge of optimization of the hybrid powertrain system so that engine and battery pack can be used in the best possible manner, thanks to a battery charging strategy allowing the diesel engine to work at its maximum efficiency point for as long as possible.

References

1. IEA (2016) Railway handbook 2016. IEA, Paris
2. Bosso N, Magelli M, Zampieri N (2020) Application of low-power energy harvesting solutions in the railway field: a review. Veh Syst Dyn 59(6):1–31
3. Key Messages for COP21 (2010) UNIFE, Brussels
4. Enno Wiebe JS (2010) Innovative integrated energy efficiency solutions for railway rolling stock, rail infrastructure and train operation. UIC-UNIFE
5. Walker AM, Lampérth MU, Wilkins S (2002) On friction braking demand with regenerative braking. SAE Trans 111:2139–2145
6. Devaux F, Tackoen X (2014) Guidelines for braking energy recovery systems in urban rail networks. Ticket to Kyoto Project
7. Clegg SJ (1996) A Review of regenerative braking systems. Dissertation, University Of Leeds
8. Jiang Y, Liu J, Tian W, Shahidehpour M, Krishnamurthy M (2014) Energy harvesting for the electrification of railway stations: getting a charge from the regenerative braking of trains. IEEE Electrification Mag 2(3):39–48
9. Cody J, Göl Ö, Nedic Z, Nafalski A, Mohtar A (2009) Regenerative braking in an electric vehicle. Electr Mach 81:113–118
10. Ghaviha N, Campillo J, Bohlin M, Dahlquist E (2017) Review of application of energy storage devices in railway transportation. Energy Procedia 105:4561–4568
11. Ogasa M (2010) Application of energy storage technologies for electric railway vehicles—examples with hybrid electric railway vehicles. IEEJ Trans Electr Electron Eng 5(3):304–311
12. King C, Vecia G, Thompson I (2015) Innovative technologies for light rail and tram: a European reference resource. INTERREG IVB North-West Europe
13. Nishimura K, Takasaki T, Sakai T (2013) Introduction of large-sized nickel–metal hydride battery GIGACELL® for industrial applications. J Alloy Compd 580(sup1):S353–S358
14. Rufer A (2010) Energy storage for railway systems, energy recovery and vehicle autonomy in Europe. In: IPEC 2010: international power electronics conference, Sapporo, Japan, 21–24 June 2010:3124–3127
15. Swanson J, Smatlak J (2015) State-of-the-art in light rail alternative power supplies. In: 13th National Light Rail and Streetcar Conference, Minneapolis, 2015:47
16. Mukai D, Kobayashi K, Kurahashi T, Matsueda N, Hashizaki K, Kogure M (2012) Development of large high-performance lithium-ion batteries for power storage and industrial use. Mitsubishi Heavy Ind Tech Rev 49(1):6–11
17. Nagaura Y, Oishi R, Shimada M, Kaneko T (2017) Battery-powered drive systems: latest technologies and outlook. Hitachi Rev 66(2):138–144
18. Barrow K (2015) Battery-electric multiple unit enters service. International Railway Journal. https://www.railjournal.com/rolling-stock/british-battery-electric-multiple-unit-enters-service/ . Accessed 13 Jan 2015
19. Chen H, Cong TN, Yang W, Tan C, Li Y, Ding Y (2009) Progress in electrical energy storage system: a critical review. Prog Nat Sci 19(3):291–312
20. Steiner M, Klohr M, Pagiela S (2007) Energy storage system with ultracaps on board of railway vehicles. In: 2007 European conference on power electronics and applications, Aalborg, 2007:1–10
21. Sitras HES-Hybrid energy storage system for rail vehicles (2010) SIEMENS
22. Moskowitz J, Cohuau J (2010) STEEM: ALSTOM and RATP experience of supercapacitors in tramway operation. In: 2010 IEEE Vehicle Power and Propulsion Conference, Lille, 2010: 1–5
23. Bolund B, Bernhoff H, Leijon M (2007) Flywheel energy and power storage systems. Renew Sustain Energy Rev 11(2):235–258
24. Hadjipaschalis I, Poullikkas A, Efthimiou V (2009) Overview of current and future energy storage technologies for electric power applications. Renew Sustain Energy Rev 13(6):1513–1522
25. Amiryar ME, Pullen KR (2017) A review of flywheel energy storage system technologies and their applications. Appl Sci 7(3):286
26. Gee AM, Dunn RW (2015) Analysis of trackside flywheel energy storage in light rail systems. IEEE Trans Veh Technol 64(9):3858–3869
27. Lee H, Jung S, Cho Y, Yoon D, Jang G (2013) Peak power reduction and energy efficiency improvement with the superconducting flywheel energy storage in electric railway system. Physica C 494:246–249
28. Spiryagin M, Wolfs P, Szanto F, Sun YQ, Cole C, Nielsen D (2015) Application of flywheel energy storage for heavy haul locomotives. Appl Energy 157:607–618
29. Rupp A, Baier H, Mertiny P, Secanell M (2016) Analysis of a flywheel energy storage system for light rail transit. Energy 107:625–638
30. Somà A, Bruzzese F, Mocera F, Viglietti E (2016) Hybridization factor and performance of hybrid electric telehandler vehicle. IEEE Trans Ind Appl 52(6):5130–5138
31. Soma A, Mocera F, Bruzzese F, Viglietti E (2016) Simulation of dynamic performances of electric-hybrid heavy working vehicles.

In: 2016 Eleventh international conference on ecological vehicles and renewable energies (EVER), Monte Carlo, 2016:1–8
32. Somà A (2017) Trends and hybridization factor for heavy-duty working vehicles. Hybrid Electr Veh. https://doi.org/10.5772/intechopen.68296
33. Mocera F, Somà A (2018) Working cycle requirements for an electrified architecture of a vertical feed mixer vehicle. Procedia Struct Integr 12:213–223
34. Bosso N, Magelli M, Zampieri N (2021) Development and validation of a new code for longitudinal train dynamics simulation. Proc Inst Mech Eng Part F: J Rail and Rapid Transit 235(3):286–299
35. Bosso N, Magelli M, Zampieri N (2020) Long train dynamic simulation by means of a new in-house code. WIT Trans Built Environ 199:249–259
36. Spiryagin M, Wu Q, Cole C (2017) International benchmarking of longitudinal train dynamics simulators: benchmarking questions. Veh Syst Dyn 55(4):450–463
37. Wu Q, Spiryagin M, Cole C, Chang C et al (2018) International benchmarking of longitudinal train dynamics simulators: results. Veh Syst Dyn 56(3):343–365
38. Rochard BP, Schmid F (2000) A review of methods to measure and calculate train resistances. Proc Ins Mech Eng Part F: J Rail and Rapid Transit 214(4):185–199
39. Spiryagin M, Cole C, Sun YQ, McClanachan M, Spiryagin V, McSweeney T (2014) Longitudinal train dynamics. In: Vantsevich VV (ed) Design and simulation of rail vehicles. CRC Press, Boca Raton, FL, pp 129–198
40. Bosso N, Magelli M, Rossi Bartoli L, Zampieri N (2021) The influence of resistant force equations and coupling system on long train dynamics simulations. Proc Inst Mech Eng, Part F: Journal of Rail and Rapid Transit. https://doi.org/10.1177/09544097211001149
41. Linden D, Reddy TB (2013) Lithium batteries. In: Linden D, Reddy TB (eds) Handbook of batteries. McGraw-Hill, New York
42. Lijun G, Shengyi L, Dougal RA (2002) Dynamic lithium-ion battery model for system simulation. IEEE Trans Compon Packag Technol 25(3):495–505
43. Tremblay O, Dessaint L, Dekkiche A (2007) A generic battery model for the dynamic simulation of hybrid electric vehicles. In: 2007 IEEE vehicle power and propulsion conference, Arlington, 2007, pp 284–289
44. Basu S, Hariharan KS, Kolake SM, Song T, Sohn DK, Yeo T (2016) Coupled electrochemical thermal modelling of a novel Li-ion battery pack thermal management system. Appl Energy 181:1–13
45. Vergori E, Mocera F, Somà A (2017) Battery modeling and simulation using a programmable testing equipment. In: 2017 9th computer science and electronic engineering (CEEC), Torino, 2017, pp 162–167
46. Mocera F, Vergori E, Somà A (2020) Battery performance analysis for working vehicle applications. IEEE Trans Ind Appl 56(1):644–653